EM 388F Term Paper: Fracture Mechanics of Delamination Buckling and Growth in Laminated Composites

Abstract

Composite laminated plates are often subject to low velocity impact which is known to cause internal ply delamination when subjected to in-plane compressive loads. This instability causes the delamination area to grow leading to an overall decrease in compressive strength of the laminated plate. This paper discusses a fracture mechanics based energy release rate approach to analyze the delamination buckling problem. Chai et. al [1] solve a simplified one-dimensional "thin film" problem where the delamination is located near the plate surface. The result of the simplified model is compared with a more general delamination depth case, solved in a similar manner, to establish its range of validity. Using a similar method and results from the one-dimensional analysis, Chai and Babcock [2] analyze compression in a laminated plate for a two-dimensional delamination.

Introduction

The high strength-to-weight ratio of fiber reinforced laminated composites makes them an attractive option in weight critical structures. The behavior of the material is more complex and less understood than traditional metals and there are concerns about long-term reliability and safety in specific areas. One of the areas of particular concern is compressive strength degradation due to an internal delamination.

Due to the low strength of a laminated plate through the thickness, an internal delamination (separation of layers) can occur due to a low velocity impact event. The size of the damage, controlled by the size of the impactor and plate dimensions, will occur in an elliptical shape as seen in figure 1. Under a critical compressive load, the delaminated area will buckle (delamination buckling) causing the damage to propagate. Characterization of the damage growth behavior under compressive load is the focus of this paper.

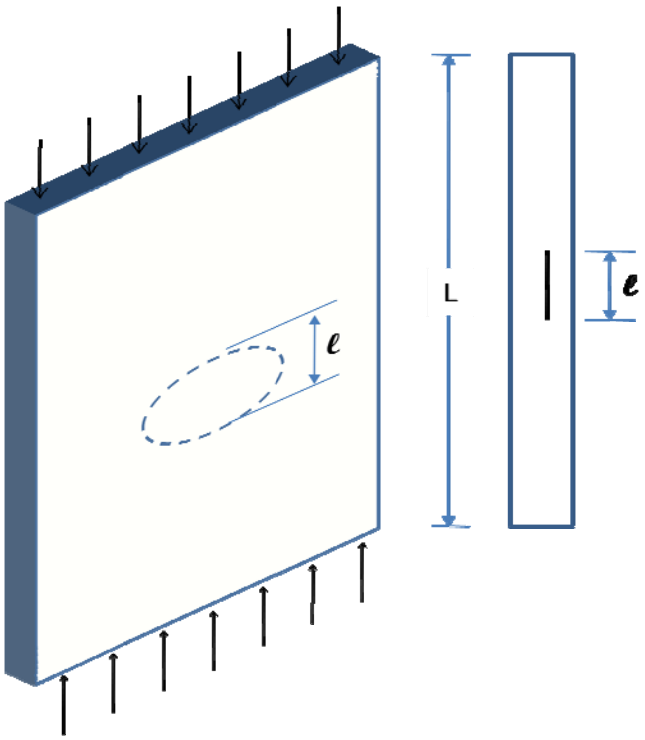

Figure 1: *Delamination under compressive load in a laminated composite plate [1]*

The analysis of the two-dimensional growth of the delamination shown in figure 1 is a highly complex problem involving elastic stability coupled with damage growth in two directions. In order to characterize this growth we first look at the one-dimensional case where a cross-section is taken of the damage. Using both a "thin-film" and general version of the damage we can analyze the different behaviors of the damage under increasing load. The delamination growth is assumed to stay within its own plane and that the size of the delamination is large compared to the thickness. Chai *et al.* [1] provide all the analysis for the one-dimensional model. The two-dimensional model of damage growth follows a similar path than that of the one-dimensional case however it is very computationally intensive. In order to characterize the damage growth we can apply specific growth cases to results from the one-dimensional case, greatly simplifying the problem. The two-dimensional analysis is taken from Chai and Babcock [2] and the results of both models are presented in the following sections.

One-Dimensional Model

In order to simplify the analysis of the damage growth due to delamination buckling we first consider a one-dimensional model of the damage. A cross section is taken through the damage as seen in figure 2 below, and using the assumption that load and geometry are constant normal to the model.

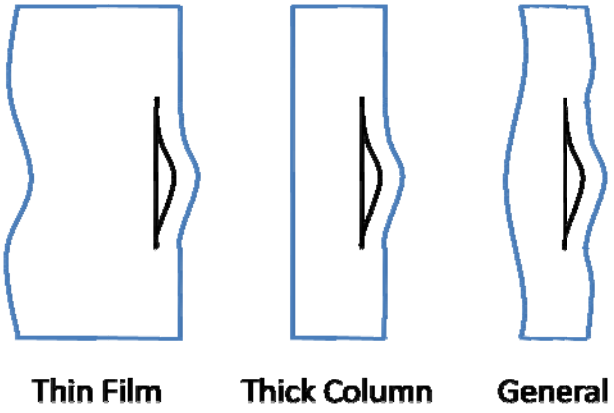

Figure 2: *One-dimensional model analysis cases [1]*

Further reducing the analysis we consider three different one-dimensional cases: "Thin-film," thick column, and general. Once again, the analyses become much more computationally intensive as the problem becomes more complicated. The "thin-film" model, the simplest case, is considered first working forward to the most general case. The results from these models are compared in order to find a range of validity for the simpler case. The "thin-film" analysis is shown in much more detail than the other cases to show the basic analysis method.

Thin-Film Model

The "thin-film" analysis is a well-known problem where the undamaged area is considered to be infinitely thick. Figure 3 shows the stages of damage in the model.

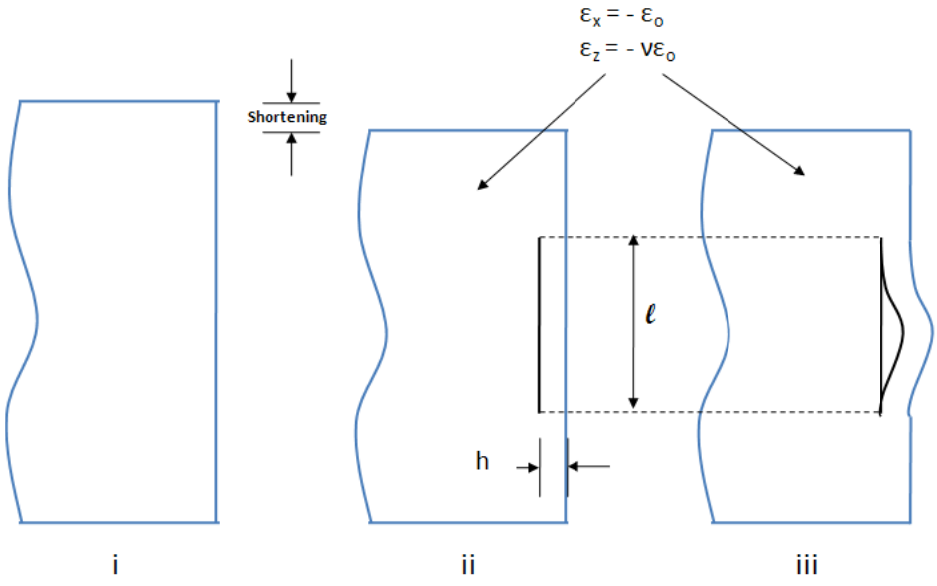

Figure 3: *Thin-film stages of damage [1]*

As shown in figure 3, stage (i) is the undamaged and unloaded structure, stage (ii) has been loaded with a strain ε_o and delamination length l has been introduced, and in stage (iii) the delamination has buckled. We see that under this compressive load, the damage can only grow if the delamination buckles. Because the strain in the undamaged infinite layer ε_o stays constant, the growth of the damage will be determined through looking at the change in energy of the buckled area.

Using beam/plate theory we find the critical strain to cause buckling,

$$\varepsilon_{cr} = \frac{\pi^2}{3(1-\nu^2)}\left(\frac{h}{l}\right)^2 . \qquad (1)$$

Assuming the undamaged area material is a 'rigid', the post-buckled film shape is,

$$y = A\frac{1}{2}\left(1+\cos\frac{2\pi x}{l}\right) \qquad . \qquad (2)$$

Because the delamination length l does not change as buckling occurs and stress in the buckled region is the buckling stress we can solve for the amplitude A.

$$\left(\varepsilon_o - \varepsilon_{cr}\right)\left(1-\nu^2\right)l = \int_{-l/2}^{l/2}\frac{1}{2}\left(\frac{dy}{dx}\right)^2 dx \qquad (3)$$

$$A^2 = \left(\varepsilon_o - \varepsilon_{cr}\right)\left(\frac{2l}{\pi}\right)^2\left(1-\nu^2\right) \qquad (4)$$

The total strain energy of the buckled region combines both the membrane and the bending strain energies (for stage iii).

$$U_{iii} = \frac{Ehl}{2}\left[\varepsilon_{cr}{}^2\left(1-\nu^2\right)+\nu^2\varepsilon_o{}^2\right]+\int_{-l/2}^{l/2}\frac{Eh^3}{24\left(1-\nu^2\right)}\left(\frac{d^2y}{dx^2}\right)^2 dx \qquad (5)$$

Simplified,

$$U_{iii} = \frac{Ehl\left(1-\nu^2\right)}{2}\left[2\varepsilon_o\varepsilon_{cr} - \varepsilon_{cr}{}^2 + \frac{\nu^2}{\left(1-\nu^2\right)}\varepsilon_o{}^2\right] \qquad (6)$$

From the total strain energy, we can simply find the energy release rate (G) as the length changes from $l \rightarrow l+\Delta l$.

$$G_a = \frac{Eh\left(1-\nu^2\right)}{2}\left(\varepsilon_o - \varepsilon_{cr}\right)\left(\varepsilon_o + 3\varepsilon_{cr}\right) \qquad (7)$$

In order for damage to propagate, the strain energy release rate must equal the fracture toughness (Γ) of the material (G/Γ = 1.0). To find the behavior of the damage growth we must first consider the energy release rate as a function of film length, shown in figure 4 below.

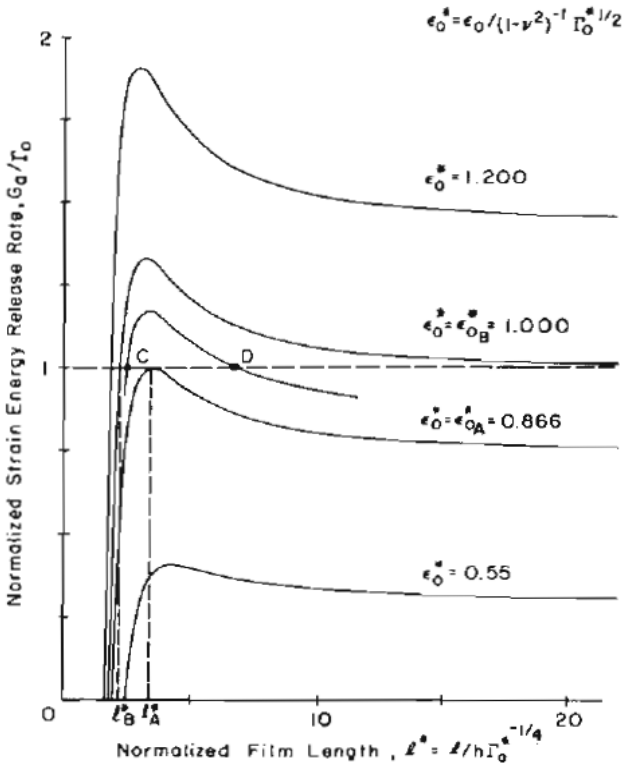

Figure 4: *Strain energy release rate as a function of film length for the "thin-film" model [1]*

To characterize the behavior of the damage growth we must first bound the problem by finding the lowest load ε_a^* (normalized) and the highest load ε_b^* that will cause growth initialization (G/Γ = 1.0). We see that each constant load curve has a local maximum, therefore the lower load bound will have a slope equal to zero when G/Γ = 1.0 . As l^* approaches infinity, the constant load curves approach a finite value. Therefore we see that the upper load bound will approach G/Γ = 1.0 as l^* increases to large values. Using these conditions, ε_a^* is determined to equal 0.866 and ε_b^* equals 1.0. Each of these load curves is associated with a length l_a^* and l_b^* (normalized) which are the lengths at first growth initiation and have values of 3.376 and 2.221 respectively.

Using the values of ε^* and l^* previously found, figure 5 below details the delamination length under load and displays trends about damage behavior.

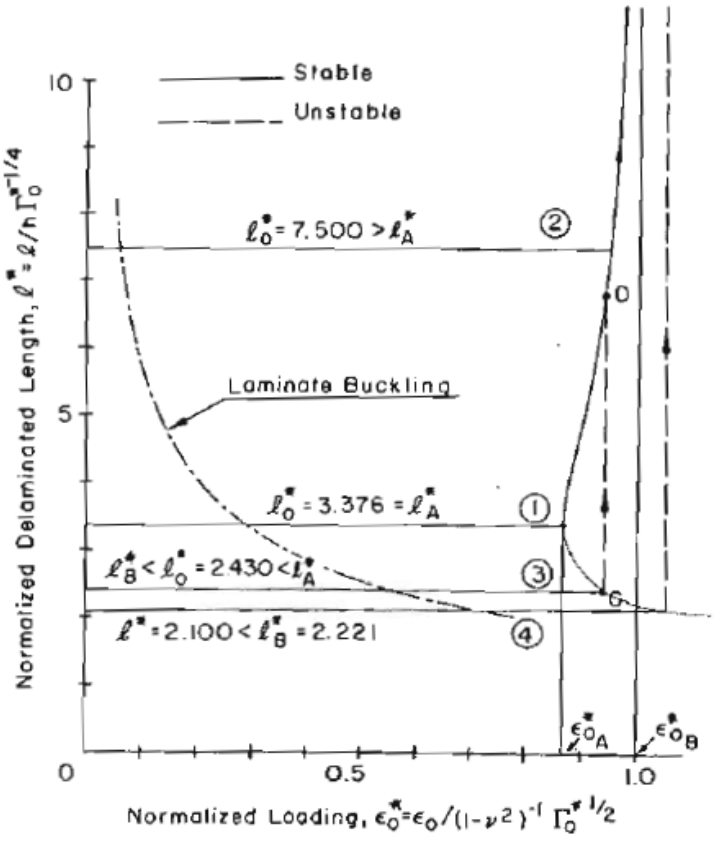

Figure 5: *Delamination length as a function of loading [1]*

To characterize the behavior of the damage growth four cases are considered. The first case has an initial delamination equal to l_a^* (3.376), as load is increased the delamination maintains a constant value until reaching ε_a^*. At this point stable growth occurs with l^* increasing to infinity as load increases. In case 2, the initial delamination is greater than l_a^* and the pattern of damage growth is the same as case 1 with a higher initiation load. Case 3 has an initial delamination between l_a^* and l_b^*. Again, growth does not occur until a load value higher than ε_a^*. When initiated, the growth in this case is unstable. Unstable growth continues until intersecting the curve at point D where stable growth occurs as l^*increases to infinity. The final case considers an initial delamination length less than l_b^*. In this case the initiation load is the highest of the cases (larger than ε_b^*) but the growth is unstable continuing to infinity. By examining these four representative cases of initial delamination length, we see that the behavior of the damage growth is highly dependent on the initial size of the damage. The shape and size of the load curve also determines how the damage will grow.

General Model

As mentioned before, the analysis of the general case of a one-dimensional beam is much more complex but follows the same method as the “thin-film”. The strain energy and energy release rate are

calculated through a numerical method as no closed form solution exists. Figure 6 below shows details of the general model.

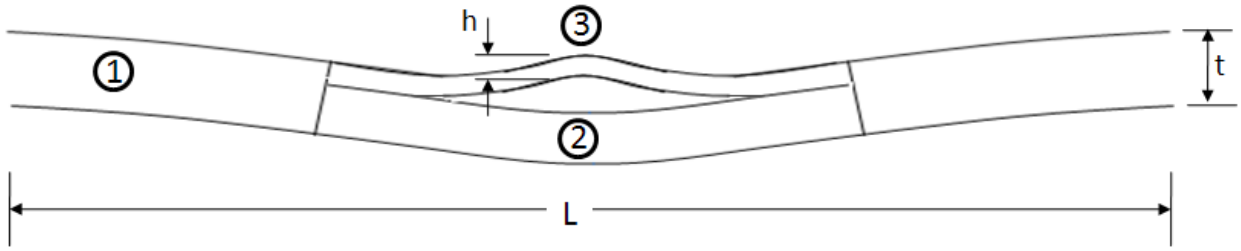

Figure 6: *One-dimensional delamination buckling general model [1]*

Each of the three sections shown in figure 6 is treated as a beam and deflections are determined using the beam equations. Compatibility and equilibrium conditions are imposed at the boundaries and each beam deflection is shown below where u_i is the normalized total load.

$$y_1 = \frac{l_1\theta}{2u_1 \sin 2u_1}\left(1-\cos\frac{2u_1x_1}{l_1}\right)$$
$$y_i = \frac{l_i\theta}{2u_i \sin u_i}\left(\cos\frac{2u_ix_i}{l_i}-\frac{\cos 2u_i}{\cos u_i}\right), i = 2,3 \qquad (8)$$

Taking the overall shortening of the plate as ε_o*L, ε_i as the midsurface strain in each segment and a constant delamination length we find the following equations,

$$\varepsilon_o L = 2\varepsilon_1 l_1 + \int_0^{l_1}\left(\frac{dy_1}{dx_1}\right)^2 dx_1 + \varepsilon_2 l_2 + \frac{1}{2}\int_{-l_2/2}^{l_2/2}\left(\frac{dy_2}{dx_2}\right)^2 dx_2 + h\theta$$
$$\varepsilon_3 l_3 + \frac{1}{2}\int_{-l_3/2}^{l_3/2}\left(\frac{dy_3}{dx_3}\right)^2 dx_3 = \varepsilon_2 l_2 + \frac{1}{2}\int_{-l_2/2}^{l_2/2}\left(\frac{dy_2}{dx_2}\right)^2 dx_2 + t\theta \qquad (9)$$

Equation (9) is essentially the same equation as equation (3) in the "thin-film" analysis. The stresses and strains in each segment are

$$(\sigma_z)_i = \frac{E\nu}{(1-\nu^2)}(\varepsilon_o - \varepsilon_i) \qquad (\sigma_x)_i = \frac{E}{(1-\nu^2)}(\nu^2\varepsilon_o - \varepsilon_i)$$
$$(\varepsilon_x)_i = -\varepsilon_i \qquad (\varepsilon_z)_i = \nu\varepsilon_o \qquad (10)$$

Using these stresses and strains we compute the strain energy as,

$$U = \left[\left(\sigma_x\right)_1\left(\varepsilon_x\right)_1 + \left(\sigma_z\right)_1\left(\varepsilon_z\right)_1\right]t_1 l_1 + D_1\int_0^{l_1}\left(\frac{d^2 y_1}{dx_1^2}\right)^2 dx_1$$
$$+\frac{1}{2}\sum_{i=2}^{3}\left\{\left[\left(\sigma_x\right)_i\left(\varepsilon_x\right)_i + \left(\sigma_z\right)_i\left(\varepsilon_z\right)_i\right]t_i l_i + D_i\int_{-l_i/2}^{l_i/2}\left(\frac{d^2 y_i}{dx_i^2}\right)^2 dx_i\right\} \qquad (11)$$

The strain energy has both membrane and bending contributions from each of the three sections of the model. Through these equations we have four unknowns (ε_1, ε_2, ε_3, and θ) with four equations to solve (equilibrium eqs, (8) and (9)). Unfortunately a closed form solution does not exist and the solution must be found using a numerical method. Once found, the unknown mid-surface strains and stresses can be used to find the total strain energy. The strain energy release rate of the system is now found using a simple numerical differentiation of the strain energy (11).

A simplification of the general model is to consider only the bending contribution of section 3 (the buckled section) giving $\theta=0^o$. This simplification gives the case of the thick column seen in figure 2 and in this case the strain energy does have a closed form solution. The process for finding this solution is the same as the "thin-film" and general models however, this result does not provide a significant difference from the "thin-film" case and will not be derived in detail.

Figure 7 below shows the energy release rate with delamination length of the three one-dimensional models at a specific delamination depth (h/t).

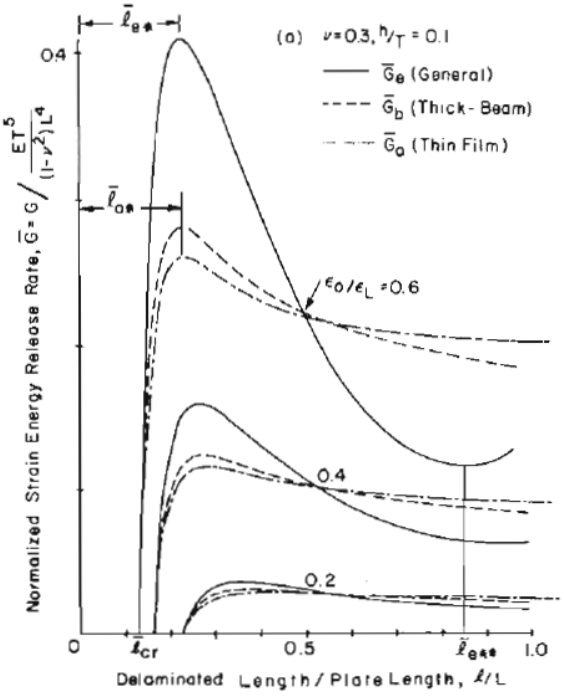

Figure 7: *Energy release rate as a function of delamination length of three models [1]*

Each set of three curves in figure 7 above show the different models at a constant load value (normalized). As seen before in the "thin-film" case each curve has a local maximum before decreasing to a minimum with rising delamination length. In order to compare the relative difference between models we compare maximum and minimum strain energy release rate values (at l_e^* and l_e^{**} for the general case). Through this method we see that the thick-column model does not greatly improve on the "thin-film" model. Focusing our attention to the general and "thin-film" models, we see that the relative difference between the maximum and minimum energy release values of the general case are much larger than the "thin-film." This relative size is important because the curve shape and size determine the stable growth behavior of the damage. In order to further examine differences between the "thin-film" and general models, figure 8 shows relative difference at various load and delamination depth of the two cases.

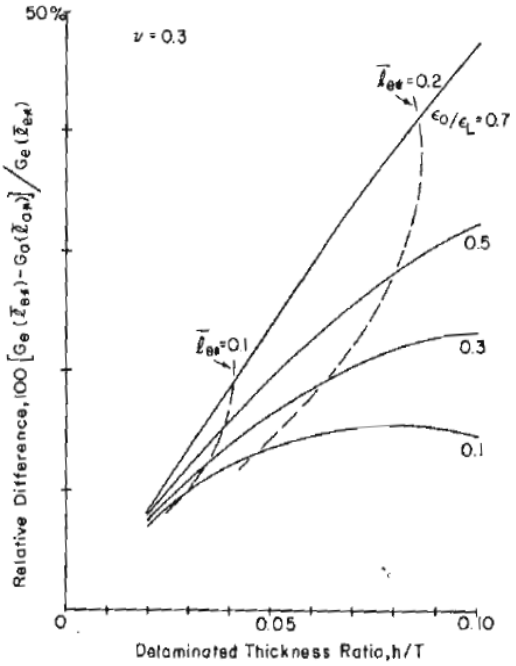

Figure 8: *Relative difference between "thin-film" and general models [1]*

Examining figure 8, the relative difference in the models clearly increases as the delamination depth (h/t) and load increases. For small depth values though the difference between the models is quite small. This result shows that the "thin-film" model can indeed be used in the place of the more general model for delaminations located near the plate surface.

Two-Dimensional Model

Expanding our scope to examine delamination in two-dimensions, we find that damage in a laminated composite from a low velocity impact typically occurs as an ellipse. In general the ellipse has major and minor axes with the possibility of damage propagation in either direction. Using the result from the one-dimensional study, delaminations in this model will be considered to be near the plate surface. Figure 9 details the damage shape and growth.

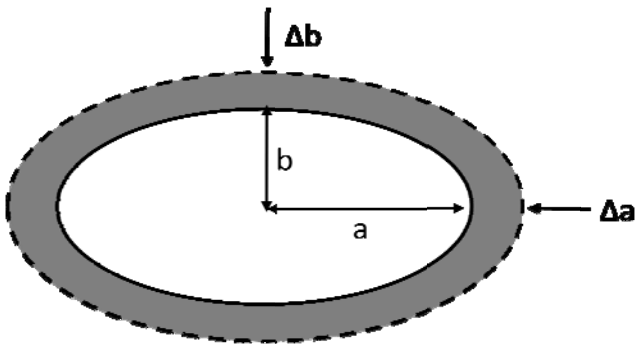

Figure 9: *Two-dimensional damage model with growth [2]*

Like the previously analyzed models, the analysis in two dimensions has both an elastic stability and delamination buckling portion. Because the focus of this paper is on the fracture mechanics of the problem and the elastic stability has a well known solution, it will not be addressed. Again, a similar energy method will be employed as that in the one-dimensional case in finding the delamination growth solution.

The strain energy release rate of the whole system (both buckled and undamaged areas) is seen as,

$$G = \frac{-d\upsilon}{dA} + G^o \qquad (12)$$

It should be noted that this approach combines all the modes of energy release rate (G). The modes of energy release rate are very hard to separate, however we expect only a small shearing effect indicating that contribution from modes II and III are minimal. Therefore G_{IC} is taken as the fracture toughness.

In equation (12) G^o is the membrane strain energy from the buckled area and further substituting for these terms gives,

$$G = \frac{G^a + G^b \frac{a}{b}\frac{db}{da}}{1 + \frac{a}{b}\frac{db}{da}} \qquad (13)$$

Where

$$G^a = \frac{-1}{\pi b}\frac{\partial U}{\partial a} + G^o$$
$$G^b = \frac{-1}{\pi b}\frac{\partial U}{\partial b} + G^o \qquad (14)$$

G^a and G^b represent relative crack driving force along each axis. These values can be easily found through differentiation of the strain energy found in the elastic stability solution. However the strain energy (13) also depends on *db/da*. This term can be found through the use of figure 10 below.

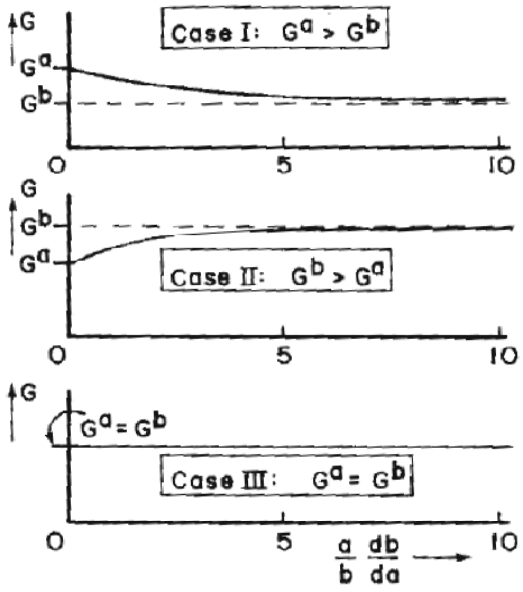

Figure 10: *db/da for relative G^a to G^b cases [2]*

To select an appropriate *db/da* value we consider the location that maximizes the energy release rate. Examining figure 10 we have three possible cases of relative G^a to G^b values. In case I where $G^a > G^b$, we see that the maximum value occurs at *db/da* = 0, substituting into (13) gives $G = G^a$. In case II where $G^b > G^a$, the maximum value occurs at *db/da* = ∞ giving $G=G^b$. However in case III there is no maximum value and *db/da* cannot be determined from the relative values. This situation will be discussed later in this paper. The G^a and G^b values in equation (14) are plotted in figure 11 below as a function of relative delamination dimensions in order to show growth behavior.

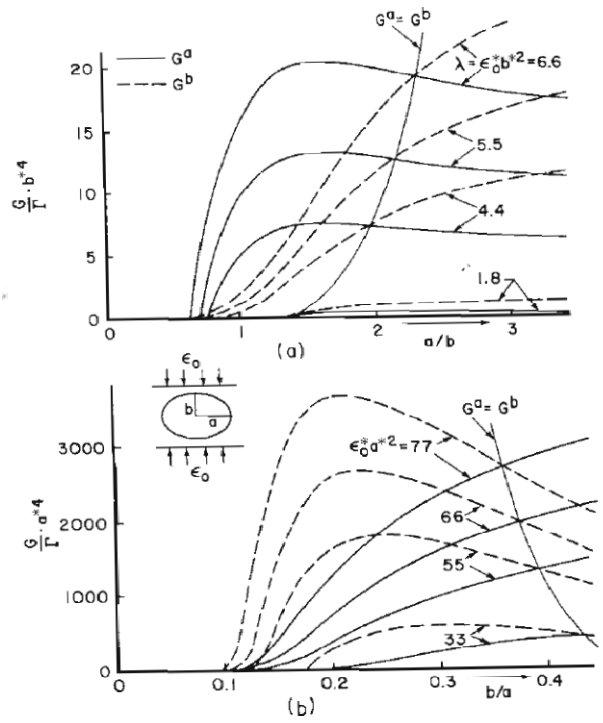

Figure 11: *G^a and G^b values as a function of relative delamination dimensions [2]*

Figure 11 shows G^a and G^b values at constant load (normalized) for changing delamination dimensions (a/b). G^a has a sharp increase to a maximum followed by decrease while G^b increases monotonically. This leads to an intersection where $G^a = G^b$. For initial values of a/b smaller than the intersection point, G^a is always greater than G^b. Because G^a is larger than G^b, we can consider this case I from figure 10 and therefore that $G=G^a$. The consequence of G equal to G^a is that crack growth will only occur in the 'a' direction. This is a very important result because the growth is one-dimensional; therefore the damage propagation behavior can be characterized in the same manner as discussed in previous sections. Conversely, if the initial a/b value is larger than the intersection point, G^b will always be greater than G^a and case II applies where $G=G^b$. The lower graph can be more useful to see case II as b/a is the delamination dimension plotted.

As previously mentioned, a problem arises when the delamination length increases and G^a approaches G^b. In this case we cannot see a distinct value for the energy release rate; this rate however is larger than the fracture toughness since the damage has already been initiated. This causes unstable crack growth in both directions due to the monotonically increasing energy release rate for a growing delamination.

Conclusion

The problem of a delamination in a compressively loaded plate has been addressed in this paper. In order to understand the complex problem, a one-dimensional model was used for computational and

analytical simplicity. The classical 'thin-film' model was compared with a more general case in order to evaluate its valid range. It was found that the 'thin-film' model gave comparable results for near surface delaminations. Additionally, the behavior of delamination growth with compressive load was characterized and found to be highly dependent on the initial size of the damage. Damage characteristics include both stable and unstable growth.

This analysis was extended to the two dimensional case where an elliptical damage was considered. By identifying areas in the two-dimensional model where the damage grows in just one direction, the behavior of a near surface delamination can be characterized as in the one-dimensional model. This powerful result indicates that the growth of a two-dimensional delamination is also highly dependent on initial damage dimensions.

Due to the simplifications used in these analyses, there is a large amount of further work that can be done in this area. For example, the fiber direction and use of other anisotropic materials may play a large role in the behavior of delamination growth. Also, an analysis for the existence of multiple delaminations at various depths is desirable to replicate actual conditions.

The analysis presented in this paper is a summary of work done in references [1] and [2].

References

1. Chai, H., Babcock, C., Knauss, W., "One Dimensional Modelling of Failure in Laminated Plates by Delamination Buckling," *International Journal of Solids and Structures*, Vol. 17, No. 11, pp. 1069-1083, 1981.
2. Chai, H., Babcock, C., "Two-Dimensional Modelling of Compressive Failure in Delaminated Laminates," *Journal of Composite Materials,* Vol. 19, No. 1, pp. 67-98, 1985.